



Comparison of the *in vitro* antibacterial activity of ofloxacin, levofloxacin, moxifloxacin, sitafloxacin, finafloxacin, and delafloxacin against *Mycobacterium tuberculosis* strains isolated in China

Yaoyao Kong^a, Zhi Geng^b, Guanglu Jiang^c, Junnan Jia^c, Fen Wang^c, Xiaoyi Jiang^c, Yuzhen Gu^c, Zhenyan Qi^a, Naihui Chu^{a,*}, Hairong Huang^{c,**}, Xia Yu^{c,**}

^a Tuberculosis Department, Beijing Chest Hospital Affiliated to Capital Medical University, Beijing, China

^b Beijing Synchrotron Radiation Facility, Institute of High Energy Physics, Chinese Academy of Sciences, Beijing, China

^c National Clinical Laboratory on Tuberculosis, Beijing Key Laboratory on Drug-Resistant Tuberculosis, Beijing Chest Hospital, Capital Medical University, Beijing, 101149, China

ARTICLE INFO

Keywords:

Mycobacterium tuberculosis
Moxifloxacin
Sitafloxacin
Delafloxacin
Antimicrobial activity
Intracellular bactericidal activity

ABSTRACT

Objective: The resistance of *Mycobacterium tuberculosis* (*Mtb*) to currently available fluoroquinolones (FQs), namely ofloxacin (OFX), levofloxacin (LFX), and moxifloxacin (MFX), renders the treatment of TB infections less successful. In this study, we aimed to evaluate the susceptibility and intracellular killing assay of *Mtb* to next-generation FQs *in vitro* and determine the correlation of FQs resistance and newly detected mutations in *gyrB* by molecular docking.

Methods: Antimicrobial susceptibility test was performed to determine the minimum inhibitory concentrations (MICs) of six FQs, including currently available FQs (OFX, LFX, and MFX) and next-generation FQs, i.e., sitafloxacin (SFX), finafloxacin (FIN) and delafloxacin (DFX) against *Mtb* clinical isolates obtained in 2015 and 2022, respectively. Quinolone-resistance-determining regions of *gyrA* and *gyrB* were subjected to DNA sequencing and the correlation of FQs resistance and new mutations in *gyrB* were determined by molecular docking. Furthermore, the intracellular antibacterial activity of the six FQs against *Mtb* H37Rv in THP-1 cells was evaluated.

Results: SFX exhibited the highest antibacterial activity against *Mtb* isolates (MIC₉₀ = 0.25 µg/mL), whereas DFX and OFX exhibited comparable activity (MIC₉₀ = 8 µg/mL). A statistically significant difference was observed among the MICs of the new generation FQs (SFX, *P* = 0.002; DFX, *P* = 0.008). Additionally, a marked increase in MICs was found in strains isolated in 2022 compared with those isolated in 2015. There might be correlation between FQs resistance and mutations in *gyrB* G520T and G520A. Cross-resistance rate between SFX and MFX was 40.6 % (26/64). At a concentration of 1 µg/mL, SFX exhibited high intracellular antibacterial activity (96.6 % ± 1.5 %) against the *Mtb* H37Rv, comparable with that of MFX at a concentration of 2 µg/mL.

Conclusion: SFX exhibits the highest inhibitory activity against *Mtb in vitro* and THP-1 cell lines, which exhibits partial-cross resistance with MFX. There might be correlation between FQs

* Corresponding author.

** Corresponding author.

*** Corresponding author.

E-mail addresses: chunaihui1994@sina.com (N. Chu), huanghairong@tb123.org (H. Huang), yuxia@mail.ccmu.edu.cn (X. Yu).

<https://doi.org/10.1016/j.heliyon.2023.e21216>

Received 23 June 2023; Received in revised form 14 September 2023; Accepted 18 October 2023

Available online 30 October 2023

2405-8440/© 2023 The Authors. Published by Elsevier Ltd. This is an open access article under the CC BY-NC-ND license (<http://creativecommons.org/licenses/by-nc-nd/4.0/>).

resistance and mutations in *gyrB* G520T and G520A. Our findings provide crucial insights into the potential clinical application of SFX and DFX in the treatment of *Mtb* infections.

1. Introduction

Tuberculosis (TB) is a major public health concern, the World Health Organization (WHO) estimates that 10.6 million new cases of TB will occur in 2021 [1]. The global incidence of multidrug-resistant TB (MDR-TB), which is characterized by resistance to both isoniazid and rifampin, is increasing. MDR-TB is often associated with poor clinical outcomes [2–4]. The WHO has recommended the use of old-generation FQs, such as OFX, LFX, and MFX, for the treatment of MDR-TB. Mounting evidence shows that there is a notable increase in the rate of MFX resistance, with figures indicating an increase from 12.9 % (41/319) in 2007 to 41.4 % (140/338) in 2013 in MDR-TB isolates in national drug resistance surveys [5]. Thus, there exists an urgent need for identifying a new generation of FQs to treat TB and to develop strategies to counteract increasing clinical drug resistance in *Mtb*.

Recently, three novel next-generation fluoroquinolones (FQs), namely sitafloxacin (SFX), moxifloxacin (MFX), and finafloxacin (FIN), were developed for potential use against MDR-TB. Sitafloxacin (SFX; Gracevit; Daiichi Sankyo, Tokyo, Japan), a synthetic broad-spectrum 8-chloro-fluoroquinolone, has been approved for the treatment of lower respiratory tract and urinary tract infections in Japan and China since 2008 and 2019, respectively [6,7]. SFX exhibits excellent distribution across various tissues, including the bronchi, alveoli, and cavities in the lung caused by TB and tissue granuloma. Furthermore, SFX exhibits a safety profile comparable with that of moxifloxacin (MFX) [8]. Compared to levofloxacin (LFX) and moxifloxacin (MFX), SFX had the lowest cumulative MIC ($MIC_{50} = 0.06 \mu\text{g/mL}$) and a relatively low ECOFF value ($0.125 \mu\text{g/mL}$) against *Mtb*. And SFX exerted stronger intracellular antibacterial activity against *Mtb* than LFX [9]. In 2015, finafloxacin (FIN), an FQ antibacterial drug, was shown to be effective in treating severe bacterial infections in slightly acidic environments [10]. FIN had a higher antibacterial activity than LFX, MFX, and ciprofloxacin between PH5.0 and 6.0 [11]. In 2017, delafloxacin (DFX; Baxdela™), an FQ antibacterial agent, was approved for its efficacy against both gram-positive and gram-negative infections [12]. Compared with other quinolones such as moxifloxacin, delafloxacin showed comparable efficacy and a lower rate of adverse effects for the treatment of respiratory and skin infections [13]. Up to now, few studies have evaluated the antibacterial activity of SFX against *Mtb in vitro*, while the antibacterial activity of FIN and DFX against *Mtb* and have not been evaluated [14,15]. The mutation related to the three novel next-generation FQs is currently unclear.

In this study, we evaluated the extent of cross-resistance among the FQs commonly employed to treat TB (i.e., ofloxacin [OFX], levofloxacin [LFX], and moxifloxacin [MFX]) at both phenotypic and genotypic levels. The objective was to assess whether current genotypic drug susceptibility assays could be used to detect resistance against the next-generation FQs (SFX, FIN, and DFX) and whether these drugs may serve as viable options for the treatment of infections caused by *Mycobacterium tuberculosis* (*Mtb*) strains that are resistant to FQs currently used to treat TB. Most cases of FQs resistance in *Mtb* are attributed to mutations within specific regions of *gyrA* and *gyrB*. Therefore, we also analyzed the trends in the resistance to the old- and next-generation FQs and mutations in *gyrA* and *gyrB* in representative isolates obtained in 2015 and 2022 at the Beijing Chest Hospital, China.

2. Materials and methods

2.1. Ethics statement

As this study only involved laboratory testing of mycobacteria and did not entail any direct involvement of human participants, ethical approval was not sought.

2.2. Study design and bacterial strains

A total of 180 *Mtb* complex strains isolated from sputum of TB patients were obtained from the National Clinical Laboratory on Tuberculosis, Beijing Chest Hospital. To determine the trends of FQ resistance, we conducted experiments at two time points across seven years (2015 and 2022). A total of 60 pan susceptible and 120 MDR-TB strains were randomly obtained in both 2015 and 2022. Of the MDR-TB strains, 60 strains were categorized as “simple MDR-TB” as they exhibited susceptibility to either FQs (OFX, LFX and MFX) or all the three second-line injectable drugs (capreomycin, kanamycin, and amikacin), whereas the other 60 strains were categorized as “MDR-TB plus” as they exhibited additional resistance to any of the FQs (OFX, LFX and MFX) and at least one of the three second-line injectable drugs. The laboratory strain *Mtb* H37Rv (ATCC 27294) was used as a quality control.

2.3. Determination of minimum inhibitory concentrations (MICs)

The six FQs evaluated in this study were purchased from Targetmol (Boston, MA, USA) and dissolved in 1 % NaOH to obtain a final concentration of 6.4 mg/mL as stock solutions; subsequently, various aliquots were prepared and stored at -70°C . We determined the MICs of OFX, LFX, MFX, FIN, and DFX by resazurin-based microplate assay [16,17]. OFX, LFX, FIN, and DFX were used at final concentrations ranging from 0.031 $\mu\text{g/mL}$ to 16 $\mu\text{g/mL}$, while MFX and SFX were used at final concentration ranging from 0.016 $\mu\text{g/mL}$ to 16 $\mu\text{g/mL}$. Briefly, *Mtb* was scraped from the Löwenstein-Jensen medium, homogenized, and adjusted to 1 McFarland turbidity standard. Then, the suspensions were further diluted (1:25) with 7H9 broth to obtain a final bacterial load of 10^5

colony-forming units (CFUs) per well. Plates were then incubated at 37 °C for seven days. Subsequently, 30 µL resazurin (0.02 %) solution was added to each well, incubation was performed for 24 h at 37 °C, and color development was assessed. An alteration in color from blue to pink or purple indicated bacterial growth MIC was defined as the lowest concentration of antibiotic that prevented a color change from blue to pink [18–20]. The pan-susceptible *Mtb* strain H37Rv (ATCC 27294) served as the control strain and included in each experiment. The critical concentration of OFX, LFX, and MFX in the 7H9 medium was 2, 1, and 0.25 µg/mL, respectively, as per the WHO's recommendations [21].

2.4. Amplification and sequencing of the *gyrA* and *gyrB* genes

We sequenced the quinolone resistance-determining regions of *gyrA* (Rv0006) and *gyrB* (Rv0005) and determined mutations relative to the sequence of the H37Rv as the reference genome [20]. For PCR, a reaction mixture (25 µL) containing 12.5 µL of 2 × Trans Taq HIFI SuperMix, 8.5 µL of nuclease-free water, 2 µL of DNA supernatant, 2 µL (20 pmol) of primers were used. The primers for *gyrA* were as follows: 5'-GACCGCAGCCACGCCAAG-3' (forward) and 5'-AGCATCACCATCGCCAACG-3' (reverse). The primers for *gyrB* were as follows: 5'-GAGTTGGTGGCGCGTAAGAGC-3' (forward) and 5'-CGGCCATCAAGCAGCATCTTG-3' (reverse). PCR was performed for 35 cycles under the following conditions: denaturation (98 °C for 30 s), annealing (55 °C for 30 s), and extension (72 °C for 30 s), and a final extension at 72 °C for 5 min. Sanger sequencing of two resistance determining regions in *gyrA* and *gyrB* were analyzed.

2.5. Molecular docking of MFX and SFX with topoisomerase II complex

There were four *gyrB* mutations detected in our study, i.e., substitutions R451S, T500 N, G520A, and G520T. The structure of the receptor of the mutated topoisomerase II complex (PDB code: 5BS8) was simulated by directly mutating corresponding amino acid residues via Coot (R451 to S451, T500 to N500, G520 to A520, and G520 to T520). To simulate the receptor and ligand and perform molecular docking of SFX, we used AutoDock Vina (version 1.2). To simulate the receptor, we eliminated all water molecules and added hydrogen atoms to the receptor structure. Subsequently, we used the Gasteiger charges model to add partial charges to the receptor via AutoDock Tools. To simulate the ligand, we assigned bond torsion as either rotatable or non-rotatable and directly saved it as a PDBQT format file [22,23].

Docking was performed with a default exhaustiveness value of 32, which denotes the number of iterations initiated with a random ligand conformation. Additionally, a default n_poses value of 9 was employed, which denotes the final number of ligand poses to be determined. To achieve a high degree of precision in the docking process, we established a suitable search box that is centered at the potential active site. As a result, the position of MFX in the PDB structure of 5BS8 was defined as the center of the cubic box with a grid size of 40 × 40 × 40 Å. To further improve the precision of the docking prediction, we repeated molecular docking multiple times. The final docking model for subsequent analysis was selected based on the predicted ligand pose with the lowest binding affinity, i.e., −18.6 kcal/mol. Receptor–ligand interactions were analyzed using LigPlot + software (version 2.2).

2.6. Intracellular killing assay and concentration kill assay

THP-1 cells were seeded in a 24-well plate (5 × 10⁵ cells per well) and subsequently differentiated using phorbol myristate acetate. Cells were infected with *Mtb* H37Rv (ATCC27294) at a multiplicity of infection (MOI) of five [24]. To eliminate extracellular bacteria, we washed the cells gently with prewarmed phosphate-buffered saline (PBS) three times 4 h post-infection. For the intracellular killing assay, RPMI complete medium containing the six FQs (OFX, LFX, MFX, SFX, FIN, and DFX) at a concentration of 1 and 2 µg/mL were added. A culture medium containing dimethyl sulfoxide (DMSO) was used as a control. Next, 1, 3, and 5 days post-infection, THP-1 cells were thoroughly washed with PBS and then lysed using 0.1 % Trion-X-100. CFUs were determined by plating serial dilutions of the lysate onto an agar medium [25,26]. The bacterial survival rate was calculated using the following formula:

$$\text{Inhibitory rate} = (\text{CFU of bacteria treated with DMSO} - \text{CFU of bacteria treated with FQs}) / \text{CFU of bacteria treated with DMSO} \times 100\%.$$

2.7. Statistical analysis

Experiments were conducted in triplicate, and each experiment included a minimum of three data points. All data were analyzed using GraphPad Prism 9.0 (GraphPad Software Inc., La Jolla, CA, USA). All tests of significance were two tailed, and a P value of 0.05 was considered statistically significant. The means of the drug-free control and drug-treated group were compared by an unpaired Student's *t*-test. The epidemiological cut-off (ECOFF) was determined according to the distribution profile of the MIC values. In cases where the MIC distribution profile was unimodal, ECOFF was defined as the concentration that inhibited 95 % of the bacterial population. In cases where the MIC distribution profile was bimodal, ECOFF was set between the two populations [27].

3. Results

3.1. Distribution of the MICs of the six FQs against *Mtb* isolates of 2015 and 2022

A total of 180 clinical *Mtb* isolates, including 60 MDR-TB strains and 30 non-MDR-TB randomly obtained in 2015 and 2022, were analyzed for *in vitro* susceptibility to old- and new-generation FQs. The MICs of OFX, LFX, MFX, SFX, FIN, and DFX against the reference strain (H37Rv) were 0.25, 0.125, 0.0625, 0.016, 0.5, and 0.25 $\mu\text{g}/\text{mL}$, respectively. The MICs of the FQs against all the isolates analyzed in this study are shown in Fig. 1(A-F).

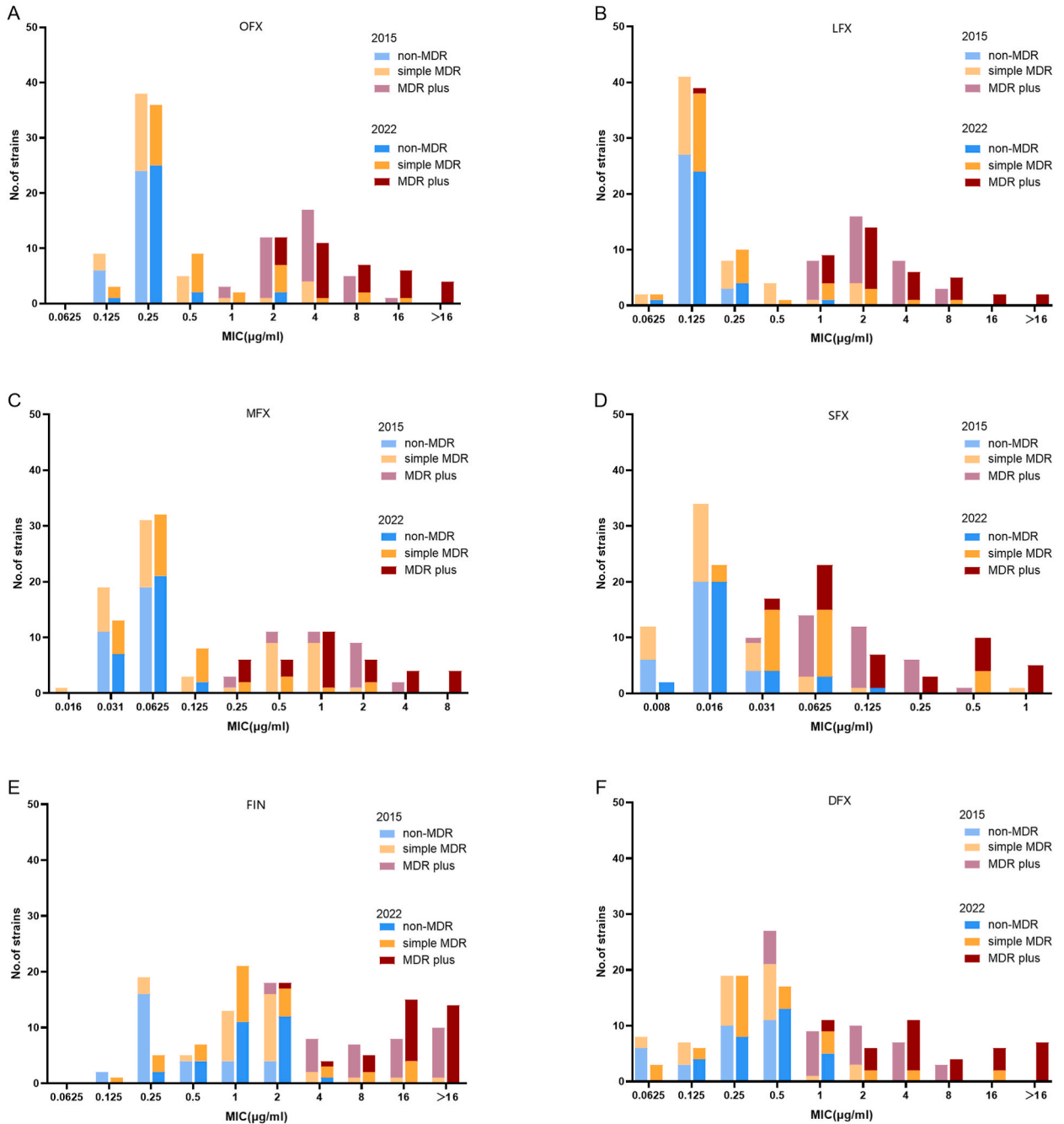


Fig. 1. The MICs distributions of six FQs (OFX,LFX,MFX,SFX, FIN and DFX) against *Mtb* isolates collected at 2015 and 2022. (A) The MICs distributions of OFX. (B) The MICs distributions of LFX. (C) The MICs distributions of MFX. (D) The MICs distributions of SFX. (E) The MICs distributions of FIN. (F) The MICs distributions of DFX.

Table 1
The MIC₅₀ and MIC₉₀ of six FQs against *Mtb* isolates.

	Total	MIC ₅₀ (µg/ml)									MIC ₉₀ (µg/ml)									
		non-MDR TB			Simple MDR-TB			MDR-TB plus			Total	non-MDR TB			Simple MDR-TB			MDR-TB plus		
		Total	2015	2022	Total	2015	2022	Total	2015	2022		Total	2015	2022	Total	2015	2022	Total	2015	2022
OFX	0.5	0.25	0.25	0.25	0.25	0.25	0.5	4	4	4	8	0.25	0.25	0.5	2	4	4	16	8	> 16
LFX	0.25	0.125	0.125	0.125	0.125	0.125	0.125	2	2	2	4	0.25	0.125	0.25	2	2	2	8	4	16
MFX	0.0625	0.0625	0.0625	0.0625	0.0625	0.0625	0.0625	1	1	1	2	0.0625	0.0625	0.0625	0.5	0.5	0.5	4	2	8
SFX	0.031	0.016	0.016	0.0625	0.031	0.016	0.0625	0.125	0.125	0.125	0.25	0.031	0.031	0.0625	0.0625	0.0625	0.5	0.5	0.25	1
FIN	2	1	0.25	1	1	2	1	16	16	16	> 16	2	2	2	8	4	16	> 16	> 16	> 16
DFX	0.5	0.25	0.25	0.25	0.25	0.25	0.25	4	2	4	8	0.5	0.5	1	2	1	4	> 16	4	> 16

Among the six FQs, SFX exhibited the highest inhibitory activity against *Mtb* isolates ($MIC_{90} = 0.25 \mu\text{g/mL}$). The MIC_{90} of SFX against non-MDR-TB, simple MDR-TB and MDR-TB plus were $0.031 \mu\text{g/mL}$, $0.0625 \mu\text{g/mL}$, $0.5 \mu\text{g/mL}$, respectively. DFX ($MIC_{90} = 8 \mu\text{g/mL}$) exhibited inhibitory activity comparable with that of OFX. The MIC_{90} of DFX against non-MDR TB, simple MDR-TB and MDR-TB plus were $0.5 \mu\text{g/mL}$, $2 \mu\text{g/mL}$, $>16 \mu\text{g/mL}$, respectively. In addition, FIN exhibited the lowest inhibitory activity ($MIC_{90} = 2 \mu\text{g/mL}$, $8 \mu\text{g/mL}$ and $>16 \mu\text{g/mL}$), whatever the drug susceptible profile was non-MDR TB, simple MDR-TB or MDR-TB plus (Table 1). Notably, a statistically significant difference in MIC was observed among the new-generation FQs (SFX, $P = 0.002$; DFX, $P = 0.008$; FIN, $P = 0.066$).

Fig. S1 shows the cumulative percentage of MIC of OFX, LFX, MFX, SFX, FIN, and DFX. The approximated cumulative % (50) values of OFX, LFX, MFX, SFX, FIN, and DFX were 0.25 and 0.5, 0.25 and 0.25, 0.0625 and 0.0625, 0.016 and 0.0625, 2 and 2, and 0.5 and 0.5 $\mu\text{g/ml/L}$ for 2015 and 2022, respectively. The approximated cumulative % (90) values of OFX, LFX, MFX, SFX, FIN, and DFX were 4 and

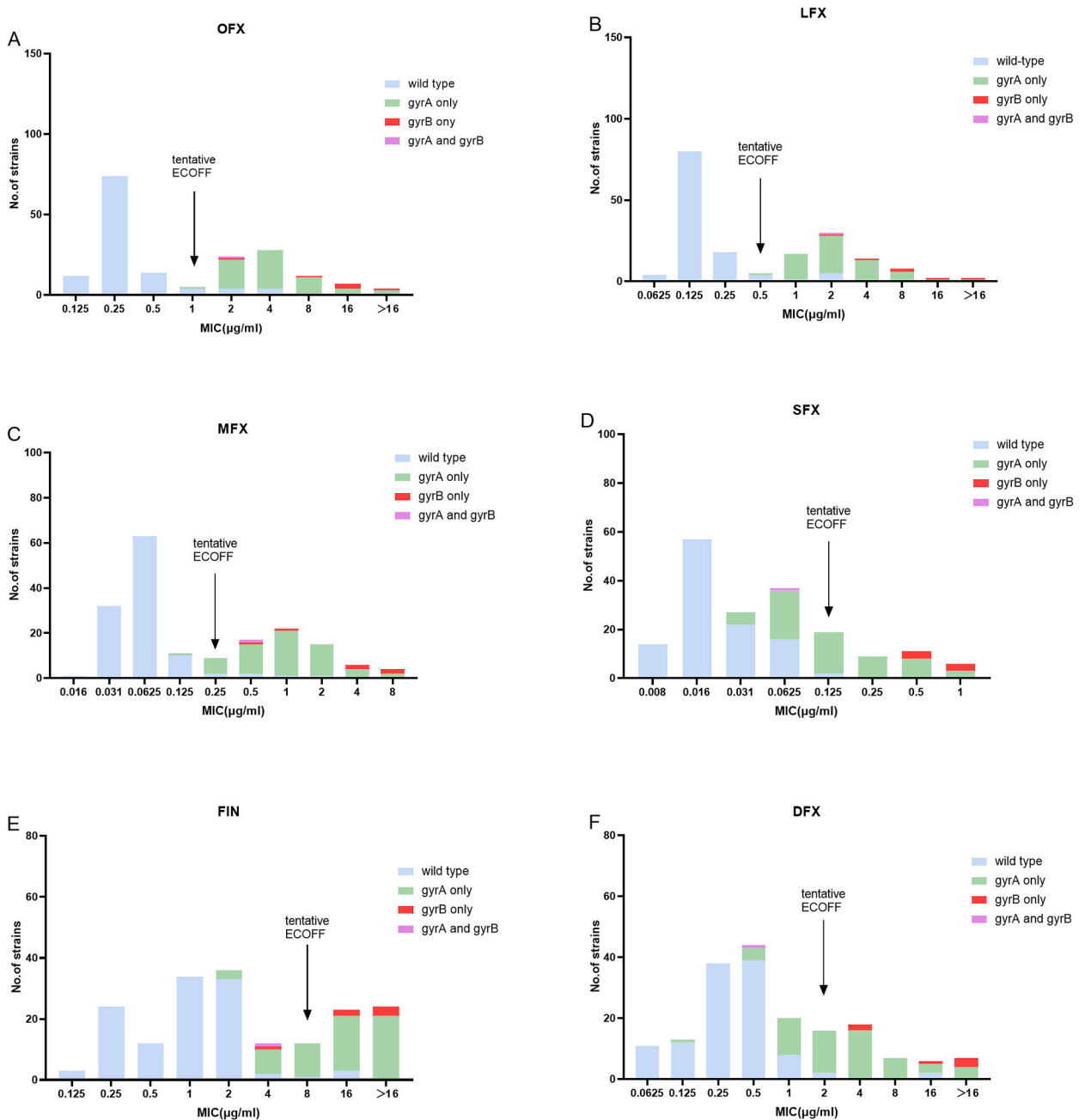


Fig. 2. The tentative ECOFF of OFX,LFX,MFX,SFX, FIN and DFX against *Mtb*. (A) The tentative ECOFF of OFX. (B) The tentative ECOFF of LFX. (C) The tentative ECOFF of MFX. (D) The tentative ECOFF of SFX. (E) The tentative ECOFF of FIN. (F) The tentative ECOFF of DFX.

16, 4 and 4, 2 and 2, 0.125 and 0.5, >16 and > 16, and 4 and 16 $\mu\text{g/mL}$ for 2015 and 2022, respectively. A notable increase in MICs was found in the strains isolated in 2022 compared with those isolated in 2015. Specifically, OFX, SFX, and DFX exhibited a four-fold increase in their MIC₉₀ values from 2015 to 2022.

3.2. Determination of ECOFF values of the FQs and cross-resistance of SFX with OFX, LFX, and MFX

The distributions of the MICs of the six FQs are shown in Fig. 2(A-F). The MICs of the six FQs exhibited a bimodal distribution, clearly segregating the phenotypic wild-type isolates from the mutant isolates. All *gyrA* mutations in the QRDR detected in this study were classical resistance mutations that resulted in an MIC increase above the tentative ECOFF for all OFX, LFX and MFX (Fig. 2A and B,C), except for *gyrA* D94A in one simple MDR-TB isolates with MIC = 0.125 $\mu\text{g/mL}$ (Fig. 2,C). The tentative ECOFF of OFX, LFX, MFX, SFX, FIN, and DFX were 1, 0.5, 0.25, 0.125, 8, and 2 $\mu\text{g/mL}$, respectively (Fig. 2). The tentative ECOFF of MFX was consistent with the breakpoint of MFX as recommended by the WHO. A total of 64 MFX-resistant isolates were detected. Considering 0.125 $\mu\text{g/mL}$ as the breakpoint for SFX, we found that the cross-resistance rate of SFX with OFX, LFX, and MFX was 49.0 % (25/51), 46.4 % (26/56), 40.6 % (26/64), respectively.

3.3. Correlations between mutations in *gyrA* and *gyrB* and MIC values

Of the strains isolated in 2015, 33 (36.67 %) strains exhibited mutations in their *gyrA* gene, such as D94 N, D94H, D94A, D94G, D94Y, A90V, S91P, and G88C. Notably, one MDR strain was observed to harbor a double mutation, i.e., A90V in *gyrA* and T500 N in *gyrB*. Of the strains isolated in 2022, 28 (31.11 %) strains exhibited mutations in their *gyrA* gene. Six MDR isolates harbored mutations in their *gyrB* gene, including five isolates with double substitutions of R451S and G520A, one isolate with G520T substitution in *gyrB* (Table S1). The aforementioned six isolates were all resistant to OFX, LFX, and MFX. In addition, the MICs of the isolates with double substitutions of R451S and G520A in the *gyrB* gene were observed to fall within the range of 0.5 and 1 $\mu\text{g/mL}$ for SFX, whereas those of the isolates with the G520T substitution in the *gyrB* genes exhibited MIC of 0.5 $\mu\text{g/mL}$. The substitutions detected in the *gyrA/gyrB* in all the isolates analyzed in this study are shown in Table S2.

3.4. Locations of the detected mutations in *gyrB*

Molecular docking of MFX and SFX with topoisomerase II complex revealed that R451, T500, and G520 were situated at a

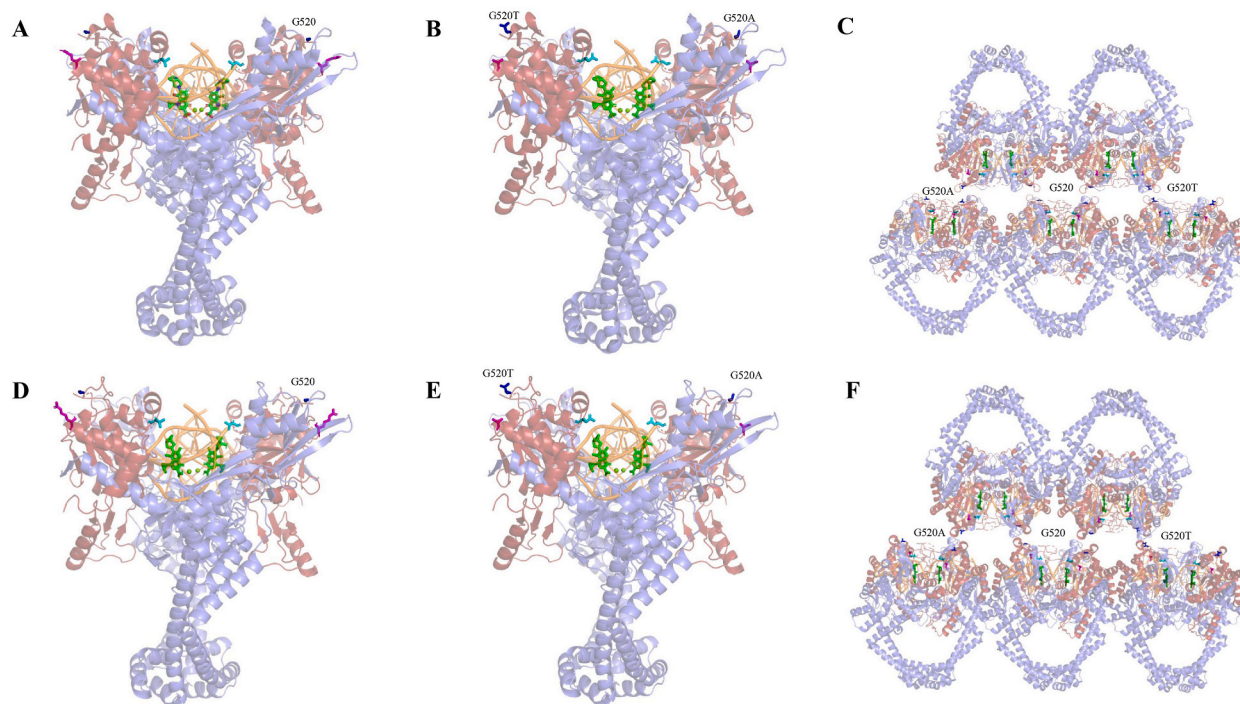


Fig. 3. Structure of the complex of *Mtb gyrA* and *gyrB* with DNA and MFX/SFX. In each panel, G520 is represented in blue, R451 in magentas, T500 in cyan, DNA in orange, and MFX/SFX in green. (A) Overall structure of the complex with *gyrB* WT and MFX. (B) Overall structure of the complex with *gyrB* R451S, G520A, and G520T and MFX. (C) Overall structure of the complex with *gyrB* R451S, G520A, G520, G520T and MFX in stack model (D) Overall structure of the complex with *gyrB* WT and SFX.(E) Overall structure of the complex with *gyrB* R451S, G520A, and G520T and SFX. (F) Overall structure of the complex with *gyrB* R451S,G520A,G520, G520T and SFX in stack model.

considerable distance from the FQ-binding sites. Modeling of *gyrB* substitution G520A and G520T showed that the primary mechanism underlying FQs resistance might be the disruption of protein polymerization in the stack model by decreasing the activity of the complex (Fig. 3,A-F).

3.5. Intracellular killing of *Mtb* by FQs

As shown in Fig. 4(A-F), the CFUs decreased upon treatment with FQs compared with DMSO at an MOI of five. After one day of incubation with OFX, LFX, MFX, SFX, FIN, and DFX at 1 $\mu\text{g}/\text{mL}$, the bacterial inhibitory rate was 17.1 % \pm 32.4 %, 54.3 % \pm 16.9 %, 82.9 % \pm 10.8 %, 96.6 % \pm 1.5 %, 65.7 % \pm 12.1 %, and 52.9 % \pm 21.5 %, respectively. Furthermore, SFX exhibited the highest inhibitory rate (98.0 % \pm 1.3 %) at a concentration of 2 $\mu\text{g}/\text{mL}$ 24 h post-treatment (Fig. 4, D). On day three, the inhibitory rate increased to 81.7 % \pm 5.9 %, 98.0 % \pm 0.8 %, 99.6 % \pm 0.2 %, 99.4 % \pm 0.3 %, 73.5 % \pm 6.5 %, 86.1 % \pm 6.5 % for OFX, LFX, MFX,

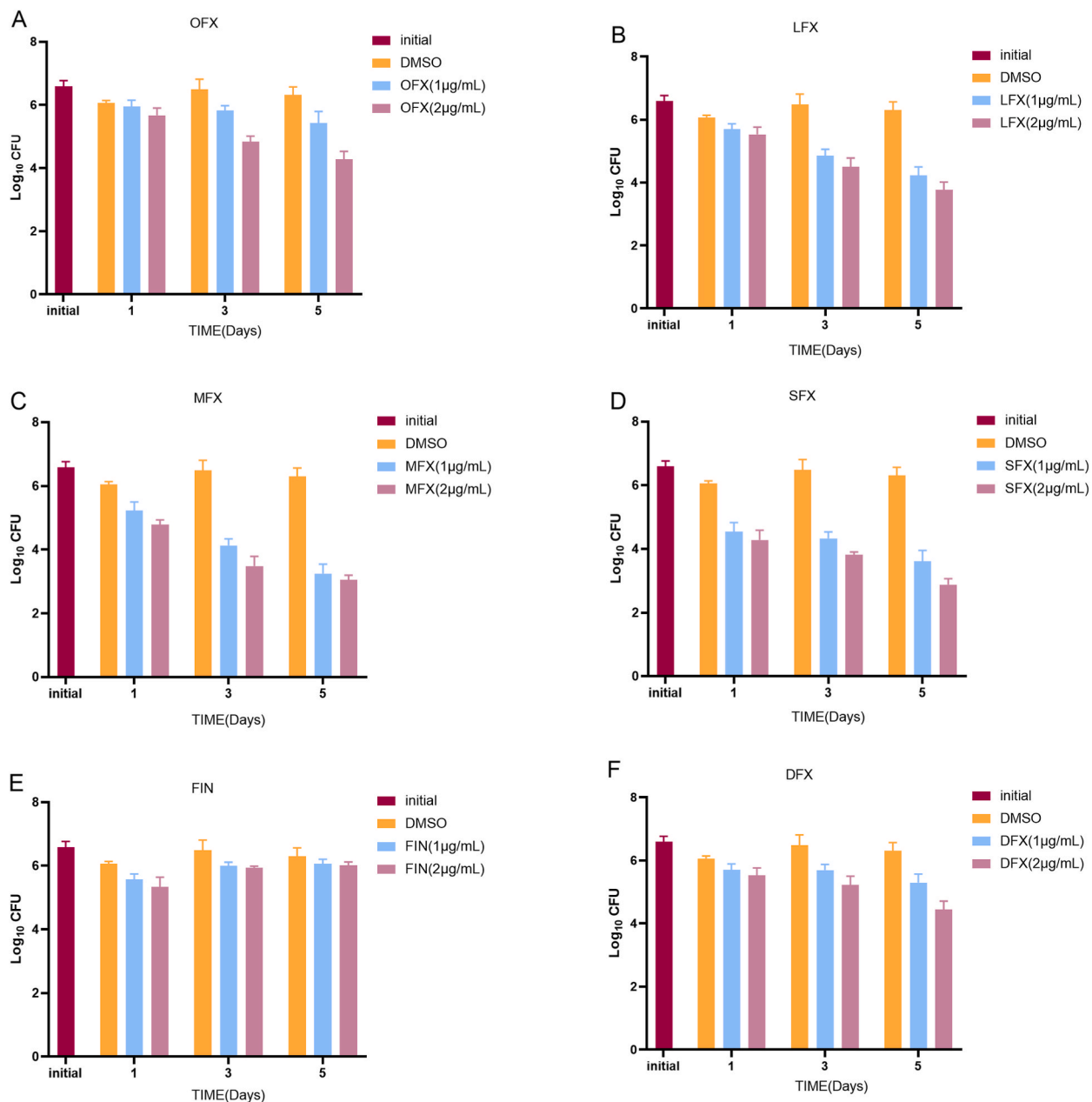


Fig. 4. Intracellular bactericidal activities of six tested FQs at different concentrations against *Mtb* in macrophages at MOI = 5; (A) OFX; (B) LFX; (C) MFX; (D) SFX; (E) FIN; (F) DFX; All data are shown as the means \pm SD (n = 5).

SFX, FIN, and DFX at a concentration of 1 µg/mL. Except for that exhibited by FIN (Fig. 4, E), the bacterial inhibitory rate exhibited by other FQs was increased five days post-infection.

4. Discussion

In this study, our findings showed that SFX exhibits the lowest MIC among the six FQs, with MIC₅₀ and MIC₉₀ values of 0.031 and 0.25 µg/mL, respectively. Notably, intracellular bacterial growth at an MOI of five was inhibited by 96.6 % ± 1.5 % following 24 h of incubation with SFX (1 µg/mL). It is consistent with other researches. One study has found that SFX exhibits a notable bactericidal effect against mycobacterium and certain nontuberculous mycobacterium (including *Mycobacterium abscessus* and *Mycobacterium avium*) [28,29]. Several studies have shown that SFX exhibits the lowest MIC compared with that of the other FQs in both drug-susceptible and drug-resistant TB [14,15]. A study involving 109 *Mtb* isolates, including 73 MDR strains, showed that the MIC₉₀ was 1 and 4 µg/mL for SFX and MFX, respectively [15]. Furthermore, based on the published area under the concentration–time curve from time zero to 24 h (AUC_{0–24}), the currently approved dose of SFX (i.e., a 200 mg daily dose) is 14.76 mg • h/L, and the fAUC_{0–24}/MIC ratio for MICs against wild-type strains (ranging from 0.031 to 0.125 µg/mL) would fall between 118 and 476 [30]. Although there is no consensus on the most optimal fAUC_{0–24}/MIC ratio that best predicts *in vivo* efficacy, ratios of 100 at the upper end of the wild-type distribution are necessary to optimize clinical outcomes [31]. In addition, SFX has been shown to exhibit a high degree of penetration into the epithelial lining fluid, with a mean penetration ratio of 0.85 following the administration of a single oral dose of 200 mg SFX in a cohort of 12 individuals [30]. Given that the currently recommended dose of SFX is notably lower than the doses of the other FQs recommended for the treatment of TB, such as the regimen containing MFX (400 mg in longer regimens or 400–800 mg in shorter regimens), the target fAUC_{0–24}/MIC of 100 at a higher dose is likely achievable; however, this supposition would have to be evaluated in clinical trials, wherein side effects would have to be monitored carefully.

Assessing cross-resistance between SFX and the current class representative is crucial. Considering 0.125 µg/mL as the breakpoint for SFX, SFX exhibited partial cross-resistance with other FQs, i.e., 49.0 % with OFX, 46.4 % with LFX, and 40.6 % with MFX, suggesting that SFX may potentially serve as a therapeutic agent for the treatment of patients with MDR-TB with resistance to MFX. A study by Yi L et al. showed that the tentative ECOFF of SFX was 0.125 µg/mL [15], which is consistent with our findings.

To the best of our knowledge, no study of the activity of DFX and FIN against *Mtb* isolates has been published. We found that DFX (MIC₉₀ = 8 µg/mL) exhibits antibacterial activity comparable with that of OFX. A study showed that DFX exhibits antibacterial activity against nontuberculous mycobacterium [32], including *Mycobacterium fortuitum* and *Mycobacterium mucogenicum* groups and *Mycobacterium kansasii*, *in vitro* with MIC₅₀ values ranging from 0.12 to 0.5 µg/mL [17]. Although the antibacterial activity of DFX is lower than that of MFX *in vitro*, DFX shows a higher level of safety than MFX. In addition, DFX exhibits a relatively mild side-effect profile, characterized by the lack of association with corrected QT (QTc) prolongation [33]. In QT studies, following the administration of therapeutic (300 mg) and supratherapeutic (900 mg) IV doses in participants (n = 52 and 51, respectively) [34], DFX did not have a clinically relevant effect on the QT/QTc interval. Thus, based on our study, DFX may serve as a potential drug for treatment.

Although *gyrA* is known to contain most common substitutions, substitutions in *gyrB* in *Mtb* clinical strains are being increasingly reported. However, the association between *gyrB* mutations and FQ resistance remains unclear. To improve the efficacy of molecular assays for the rapid detection of FQ resistance in *Mtb*, clarifying the molecular basis of the resistance against FQs is crucial. Herein, the prevalence of *gyrB* mutations associated with FQs resistance in *Mtb* was found to range from 1.10 % (1/90) in 2015 to 6.67 % (6/90) in 2022. Four *gyrB* substitutions, namely T539 N, R451S, G520A and G520T, were detected. T539 substitutions in *gyrB*, such as T539A, T539P, and T539 N, have been widely reported in cases of FQ resistance [35–37]. In contrast, R451S, G520A, and G520T substitutions have not been reported in association with FQ resistance. Notably, these three substitutions were detected in MFX-resistant isolates exhibiting MIC of 0.5–8 µg/mL, including double substitutions of R451S and G520A (n = 5) and G520T (n = 1). As per the simulated structure of *gyrB* and MFX, R451 and G520 were located at a considerable distance from MFX, suggesting that the mechanism underlying the corresponding resistance may not be due to a direct interaction between the drug and its target. G520A and G520T in *gyrB* may disrupt the polymerization of the complex via stack docking [38], which may lead to MFX-resistance in the above five *Mtb* isolates.

Among the isolates harboring *gyrB* mutations in this study, a notable cross-resistance was observed between MFX and SFX for R451S, G520A and G520T *gyrB* mutations, whereas T500 N *gyrB* mutation was observed to be susceptible to SFX and resistant to MFX. Thus, SFX may be active against strains with specific mutations of *gyrB*, indicating the potential use of SFX in cases of resistance to old-generation FQs, such as OFX, LFX, and MFX.

Our study has several limitations. First, the sample size was small. Second, all the *Mtb* isolates analyzed in this study were obtained from one hospital, i.e., the Beijing Chest Hospital, a designated clinical center on TB that attracts patients with TB from all over the country. Nonetheless, many isolates may be genetically and epidemiologically related; therefore, more clinical isolates are needed to assess the resistance rate across diverse epidemiological backgrounds.

In conclusion, SFX exhibits the highest inhibitory activity against *Mtb in vitro* and intracellular exhibits partial-cross resistance with MFX. There might be correlation between FQs resistance and mutations in *gyrB* G520T and G520A. Our findings provide crucial insights into the potential clinical application of SFX and DFX in the treatment of *Mtb* infections.

Funding

This study was supported by research funding from the Natural Science Fund of China (82072328), Beijing Public Health Experts Project (grant number G2023-2-002 and G2023-3-004), Beijing Hospitals Authority Youth Programme (QML20211602) and Tongzhou “Yun He” Talent Project (YHLD2019001).

Declaration of competing interest

The authors declare that they have no known competing financial interests or personal relationships that could have appeared to influence the work reported in this paper.

Appendix A. Supplementary data

Supplementary data to this article can be found online at <https://doi.org/10.1016/j.heliyon.2023.e21216>.

References

- [1] World Health Organization, Global Tuberculosis Report 2022, 2022. https://www.who.int/tb/publications/global_report/en/.
- [2] N. Ahmad, S.D. Ahuja, O.W. Akkerman, J.C. Alffenaar, L.F. Anderson, P. Baghaei, D. Bang, P.M. Barry, M.L. Bastos, D. Behera, A. Benedetti, G.P. Bisson, M. J. Boeree, M. Bonnet, S.K. Brode, J.C.M. Brust, Y. Cai, E. Caumes, J.P. Cegielski, R. Centis, P.C. Chan, E.D. Chan, K.C. Chang, M. Charles, A. Cirule, M. P. Dalcolmo, L. D'Ambrosio, G. de Vries, K. Dheda, A. Esmail, J. Flood, G.J. Fox, M. Fréchet-Jachym, G. Fregona, R. Gayoso, M. Gegia, M.T. Gler, S. Gu, L. Guglielmetti, T.H. Holtz, J. Hughes, P. Isaakidis, L. Jarlsberg, R.R. Kempker, S. Keshavjee, F.A. Khan, M. Kipiani, S.P. Koenig, W.J. Koh, A. Kritski, et al., Treatment correlates of successful outcomes in pulmonary multidrug-resistant tuberculosis: an individual patient data meta-analysis, *Lancet* 392 (2018) 821–834, [https://doi.org/10.1016/S0140-6736\(18\)31644-1](https://doi.org/10.1016/S0140-6736(18)31644-1).
- [3] Y. Li, F. Sun, W. Zhang, Bedaquiline and delamanid in the treatment of multidrug-resistant tuberculosis: promising but challenging, *Drug Dev. Res.* 80 (2019) 98–105, <https://doi.org/10.1002/ddr.21498>.
- [4] A. Alemu, Z.W. Bitew, T. Worku, Poor treatment outcome and its predictors among drug-resistant tuberculosis patients in Ethiopia: a systematic review and meta-analysis, *Int. J. Infect. Dis.* 98 (2020) 420–439, <https://doi.org/10.1016/j.ijid.2020.05.087>.
- [5] H. Xia, Y. Zheng, D. Liu, S. Wang, W. He, B. Zhao, Y. Song, X. Ou, Y. Zhou, S. van den Hof, F. Cobelens, Y. Zhao, Strong increase in moxifloxacin resistance rate among multidrug-resistant mycobacterium tuberculosis isolates in China, 2007 to 2013, *Microbiol. Spectr.* 9 (2021), e0040921, <https://doi.org/10.1128/Spectrum.00409-21>.
- [6] G.M. Keating, Sitafloxacin: in bacterial infections, *Drugs* 71 (2011) 731–744, <https://doi.org/10.2165/11207380-000000000-00000>.
- [7] S. Guo, X. Li, Y. Li, H. Tong, M. Wei, B. Yan, M. Tian, B. Xu, J. Shao, Sitafloxacin pharmacokinetics/pharmacodynamics against multidrug-resistant bacteria in a dynamic urinary tract infection in vitro model, *J. Antimicrob. Chemother.* 78 (2022) 141–149, <https://doi.org/10.1093/jac/dkac365>.
- [8] Y. Li, D. Zhu, Y. Peng, Z. Tong, Z. Ma, J. Xu, S. Sun, H. Tang, Q. Xiu, Y. Liang, X. Wang, X. Lv, Y. Dai, Y. Zhu, Y. Qu, K. Xu, Y. Huang, S. Wu, G. Lai, X. Li, X. Han, Z. Yang, J. Sheng, Z. Liu, H. Li, Y. Chen, H. Zhu, Y. Zhang, A randomized, controlled, multicenter clinical trial to evaluate the efficacy and safety of oral sitafloxacin versus moxifloxacin in adult patients with community-acquired pneumonia, *Curr. Med. Res. Opin.* 37 (2021) 693–701, <https://doi.org/10.1080/03007995.2021.1885362>.
- [9] L. Yi, A. Aono, K. Chikamatsu, Y. Igarashi, H. Yamada, A. Takaki, S. Mitarai, In vitro activity of sitafloxacin against mycobacterium tuberculosis with gyrA/B mutations isolated in Japan, *J. Med. Microbiol.* 66 (2017) 770–776, <https://doi.org/10.1099/jmm.0.000493>.
- [10] K. McKeage, Finafloxacin: first global approval, *Drugs* 75 (2015) 687–693, <https://doi.org/10.1007/s40265-015-0384-z>.
- [11] W. Stubbings, P. Leow, G.C. Yong, F. Goh, B. Körber-Irrgang, M. Kresken, R. Endermann, H. Labischinski, In vitro spectrum of activity of finafloxacin, a novel, pH-activated fluoroquinolone, under standard and acidic conditions, *Antimicrob. Agents Chemother.* 55 (2011) 4394–4397, <https://doi.org/10.1128/AAC.00833-10>.
- [12] A. Markham, Delafloxacin: first global approval, *Drugs* 77 (2017) 1481–1486, <https://doi.org/10.1007/s40265-017-0790-5>.
- [13] M. Bassetti, P. Della Siega, D. Pecori, C. Scarparo, E. Righi, Delafloxacin for the treatment of respiratory and skin infections, *Expert Opin. Invest. Drugs* 24 (2015) 433–442, <https://doi.org/10.1517/13543784.2015.1005205>.
- [14] M. Leechawengwongs, T. Prammananan, S. Jaitrong, P. Billamas, N. Makhao, N. Thamngongdee, A. Thanormchat, A. Phurattanakornkul, S. Rattanarangsee, C. Ratanajaraya, A. Disrathakit, A. Chairpasert, In vitro activity and MIC of sitafloxacin against multidrug-resistant and extensively drug-resistant mycobacterium tuberculosis isolated in Thailand, *Antimicrob. Agents Chemother.* 62 (2018), <https://doi.org/10.1128/AAC.00825-17>.
- [15] L. Yi, A. Aono, K. Chikamatsu, Y. Igarashi, H. Yamada, A. Takaki, S. Mitarai, In vitro activity of sitafloxacin against mycobacterium tuberculosis with gyrA/B mutations isolated in Japan, *J. Med. Microbiol.* 66 (2017) 770–776, <https://doi.org/10.1099/jmm.0.000493>.
- [16] N. Coeck, B.C. de Jong, M. Diels, P. de Rijk, E. Ardizzoni, A. Van Deun, L. Rigouts, Correlation of different phenotypic drug susceptibility testing methods for four fluoroquinolones in mycobacterium tuberculosis, *J. Antimicrob. Chemother.* 71 (2016) 1233–1240, <https://doi.org/10.1093/jac/dkv499>.
- [17] B.A. Brown Elliott, R.J. Wallace, Jr, Comparison of in vitro susceptibility of delafloxacin with ciprofloxacin, moxifloxacin, and other comparator antimicrobials against isolates of nontuberculous mycobacteria, *Antimicrob. Agents Chemother.* 65 (2021), e0007921, <https://doi.org/10.1128/AAC.00079-21>.
- [18] B. Lopez, R. Siqueira de Oliveira, J.M.W. Pinhata, E. Chimara, E. Pacheco Ascencio, Z.M. Puyén Guerra, I. Wainmayer, N. Simboli, M. Del Granado, J. C. Palomino, V. Ritacco, A. Martin, Bedaquiline and linezolid MIC distributions and epidemiological cut-off values for mycobacterium tuberculosis in the Latin American region, *J. Antimicrob. Chemother.* 74 (2019) 373–379, <https://doi.org/10.1093/jac/dky414>.
- [19] Y. Pang, Z. Zong, F. Huo, W. Jing, Y. Ma, L. Dong, Y. Li, L. Zhao, Y. Fu, H. Huang, In vitro drug susceptibility of bedaquiline, delamanid, linezolid, clofazimine, moxifloxacin, and gatfloxacin against extensively drug-resistant tuberculosis in Beijing, China, *Antimicrob. Agents Chemother.* 61 (2017), <https://doi.org/10.1128/AAC.00900-17>.
- [20] X. Yu, G. Wang, S. Chen, G. Wei, Y. Shang, L. Dong, T. Schön, D. Moradigaravand, J. Parkhill, S.J. Peacock, C.U. Köser, H. Huang, Wild-type and non-wild-type mycobacterium tuberculosis MIC distributions for the novel fluoroquinolone antofloxacin compared with those for ofloxacin, levofloxacin, and moxifloxacin, *Antimicrob. Agents Chemother.* 60 (2016) 5232–5237, <https://doi.org/10.1128/AAC.00393-16>.
- [21] Anonymous, Updating the approaches to define susceptibility and resistance to anti-tuberculosis agents: implications for diagnosis and treatment, *Eur. Respir. J.* 59 (2022), 2200166, <https://doi.org/10.1183/13993003.00166-2022>.
- [22] G.M. Morris, R. Huey, W. Lindstrom, M.F. Sanner, R.K. Belew, D.S. Goodsell, A.J. Olson, AutoDock4 and AutoDockTools4: automated docking with selective receptor flexibility, *J. Comput. Chem.* 30 (2009) 2785–2791, <https://doi.org/10.1002/jcc.21256>.
- [23] O. Trott, A.J. Olson, AutoDock Vina: improving the speed and accuracy of docking with a new scoring function, efficient optimization, and multithreading, *J. Comput. Chem.* 31 (2010) 455–461, <https://doi.org/10.1002/jcc.21334>.
- [24] F. Liu, J. Chen, P. Wang, H. Li, Y. Zhou, H. Liu, Z. Liu, R. Zheng, L. Wang, H. Yang, Z. Cui, F. Wang, X. Huang, J. Wang, W. Sha, H. Xiao, B. Ge, MicroRNA-27a controls the intracellular survival of mycobacterium tuberculosis by regulating calcium-associated autophagy, *Nat. Commun.* 9 (2018) 4295, <https://doi.org/10.1038/s41467-018-06836-4>.
- [25] S. Chen, T. Teng, Z. Zhang, Y. Shang, H. Xiao, G. Jiang, F. Wang, J. Jia, L. Dong, L. Zhao, N. Chu, H. Huang, Carbonyl Cyanide 3-Chlorophenylhydrazone (CCCP) exhibits direct antibacterial activity against mycobacterium abscessus, *Infect. Drug Resist.* 14 (2021) 1199–1208, <https://doi.org/10.2147/IDR.S303113>.
- [26] R. Zhu, Y. Shang, S. Chen, H. Xiao, R. Ren, F. Wang, Y. Xue, L. Li, Y. Li, N. Chu, H. Huang, In vitro activity of the sudapyridine (WX-081) against non-tuberculous mycobacteria isolated in Beijing, China, *Microbiol. Spectr.* 10 (2022), e0137222, <https://doi.org/10.1128/spectrum.01372-22>.

- [27] X. Yu, X. Gao, C. Li, J. Luo, S. Wen, T. Zhang, Y. Ma, L. Dong, F. Wang, H. Huang, In vitro activities of bedaquiline and delamanid against nontuberculous mycobacteria isolated in Beijing, China, *Antimicrob. Agents Chemother.* 63 (2019), <https://doi.org/10.1128/AAC.00031-19>.
- [28] S. He, Q. Guo, L. Zhao, L. Xu, J. Fan, W. Wu, Z. Zhang, B. Li, H. Chu, Sitaflloxacin expresses potent anti-mycobacterium abscessus activity, *Front. Microbiol.* 12 (2021), 779531, <https://doi.org/10.3389/fmicb.2021.779531>.
- [29] C. Sano, Y. Tatano, T. Shimizu, S. Yamabe, K. Sato, H. Tomioka, Comparative in vitro and in vivo antimicrobial activities of sitafloxacin, gatifloxacin and moxifloxacin against mycobacterium avium, *Int. J. Antimicrob. Agents* 37 (2011) 296–301, <https://doi.org/10.1016/j.ijantimicag.2010.12.014>.
- [30] T. Paiboonvong, W. Nosoongnoen, K. Sathirakul, V. Tangsujaritvijit, J. Kaemapairoj, P. Tragulpiankit, P. Montakantikul, Pharmacokinetics and penetration of sitafloxacin into alveolar epithelial lining fluid in critically ill Thai patients with pneumonia, *Antimicrob. Agents Chemother.* 63 (2019), <https://doi.org/10.1128/AAC.00800-19>.
- [31] A.D. Pranger, J.W. Alffenaar, R.E. Aarnoutse, Fluoroquinolones, the cornerstone of treatment of drug-resistant tuberculosis: a pharmacokinetic and pharmacodynamic approach, *Curr. Pharmaceut. Des.* 17 (2011) 2900–2930, <https://doi.org/10.2174/138161211797470200>.
- [32] K.L. Chew, S. Octavia, J. Go, S.F. Yeoh, J. Teo, MIC Distributions of routinely tested antimicrobials and of rifabutin, eravacycline, delafloxacin, clofazimine, and bedslraquinile for mycobacterium fortuitum, *Antimicrob. Agents Chemother.* 65 (2021), e0059321, <https://doi.org/10.1128/AAC.00593-21>.
- [33] J. Shiu, G. Ting, T.K. Kiang, Clinical Pharmacokinetics and pharmacodynamics of delafloxacin, *Eur. J. Drug Metab. Pharmacokinet.* 44 (2019) 305–317, <https://doi.org/10.1007/s13318-018-0520-8>.
- [34] J.S. Litwin, M.S. Benedict, M.D. Thorn, L.E. Lawrence, S.K. Cammarata, E. Sun, A thorough QT study to evaluate the effects of therapeutic and supratherapeutic doses of delafloxacin on cardiac repolarization, *Antimicrob. Agents Chemother.* 59 (2015) 3469–3473, <https://doi.org/10.1128/AAC.04813-14>.
- [35] E.Y. Nosova, A.A. Bukatina, Y.D. Isaeva, M.V. Makarova, K.Y. Galkina, A.M. Moroz, Analysis of mutations in the gyrA and gyrB genes and their association with the resistance of mycobacterium tuberculosis to levofloxacin, moxifloxacin and gatifloxacin, *J. Med. Microbiol.* 62 (2013) 108–113, <https://doi.org/10.1099/jmm.0.046821-0>.
- [36] A. Pantel, S. Petrella, N. Veziris, F. Brossier, S. Bastian, V. Jarlier, C. Mayer, A. Aubry, Extending the definition of the GyrB quinolone resistance-determining region in mycobacterium tuberculosis DNA gyrase for assessing fluorquinolone resistance in, M. tuberculosis. *Antimicrob Agents Chemother* 56 (2012) 1990–1996, <https://doi.org/10.1128/AAC.06272-11>.
- [37] L.L. Zhao, Q. Sun, C.Y. Zeng, Y. Chen, B. Zhao, H.C. Liu, Q. Xia, X.Q. Zhao, W.W. Jiao, G.L. Li, K.L. Wan, Molecular characterisation of extensively drug-resistant mycobacterium tuberculosis isolates in China, *Int. J. Antimicrob. Agents* 45 (2015) 137–143, <https://doi.org/10.1016/j.ijantimicag.2014.09.018>.
- [38] L. Sonnenkalb, J.J. Carter, A. Spitaleri, Z. Iqbal, M. Hunt, K.M. Malone, C. Utpatel, D.M. Cirillo, C. Rodrigues, K.S. Nilgiriwala, P.W. Fowler, M. Merker, S. Niemann, Bedaquiline and clofazimine resistance in mycobacterium tuberculosis: an in-vitro and in-silico data analysis, *Lancet Microbe* 4 (2023) e358–e368, [https://doi.org/10.1016/S2666-5247\(23\)00002-2](https://doi.org/10.1016/S2666-5247(23)00002-2).